1694 *Organometallics* **1984**, *3*, 1694–1706

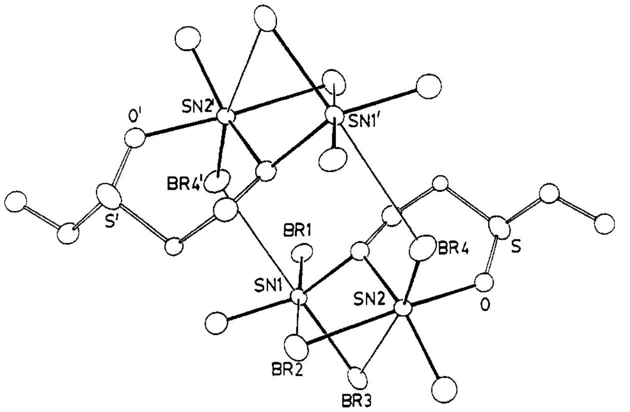

Figure 5. Schematic representation of tetranuclear 3,3-bis(dibromomethylstannyl)propyl ethyl sulfoxide [$(Br_2MeSn)_2CHCH_2CH_2S(O)Et$], 4.

and angles for the four compounds of this study. Tables of anisotropic thermal parameters calculated hydrogen positions, and observed and calculated structure factor amplitude are provided as supplementary materials. Views of the molecular geometries along with the atom-labeling scheme are shown in Figures 1–5.

Acknowledgment. We are grateful for support of this research by the National Science Foundation (Grants CHE 780075402 and CHE 8105020) and by the National Institutes of Health (partially by Grant GM 22566 and funding for the diffractometer from Grant GM 27459). Acknowledgment is also made to the donors of the Petroleum Research Fund, administered by the American Chemical Society, for partial support. We thank Mr. Jon Hayes for assistance with the graphics.

Registry No. 1, 91230-55-6; 2, 91230-56-7; 3, 91230-57-8; 4, 91230-58-9; $(Me_3Sn)_2CHCH_2CH_2SOEt$, 85294-03-7.

Supplementary Material Available: Tables of anisotropic thermal parameters calculated hydrogen positions and isotropic thermal parameters, and calculated and observed structure factors for compounds 1–4 (45 pages). Ordering information is given on any current masthead page.

Reactions of Atomic Cobalt Ions with Aldehydes and Ketones. Observation of Decarbonylation Processes Leading to Formation of Metal Alkyls and Metallacycles in the Gas Phase†

L. F. Halle, W. E. Crowe,[1a] P. B. Armentrout,[1b] and J. L. Beauchamp*

Arthur Amos Noyes Laboratory of Chemical Physics, California Institute of Technology,
Pasadena, California 91125

Received December 19, 1983

An ion beam apparatus is used to study the reactions of singly charged cobalt positive ions with several aldehydes and ketones as a function of relative kinetic energy. Deuterium labeling is used to provide mechanistic information. Decarbonylation yielding $CoCO^+$ is the dominant process in the reactions of Co^+ with formaldehyde, acetaldehyde, and acetone at low energies. At ~0.5 eV relative kinetic energy cross sections for formation of $CoCO^+$ from these neutrals are 0.25, 29, and 80 Å^2, respectively, indicating that formaldehyde is much less reactive than the alkyl-substituted species. An ion corresponding to $Co(CH_3)_2^+$ is formed as an exothermic product in the reaction of Co^+ with acetone. The analogous product is also observed in the reactions of Fe^+ and Ni^+ with acetone. This indicates that the sum of the first two methyl bond energies to first-row group 8 metal ions is greater than 96 kcal/mol, which exceeds typical C–C single bond energies and supports the conclusion of earlier studies that metal ion insertion into unactivated carbon–carbon bonds of saturated hydrocarbons is an exothermic process. As the alkyl chains of the dialkyl ketones are extended, loss of alkene and aldehyde dominate the product distributions at low energies. If one of the alkyl groups is highly branched, the major product is due to loss of methane. Decarbonylation of cyclopentanone yields $Co(C_4H_8)^+$, suggested to be a metallacycle which further dehydrogenates to yield $Co(C_4H_6)^+$ as the major species formed in exothermic processes at low relative kinetic energies. Analyses of products formed at high relative kinetic energies are used in conjunction with thermochemical estimates to infer mechanistic details and construct qualitative reaction coordinate diagrams for the interaction of metal ions with carbonyl compounds. Some interesting conclusions can be reached from an inspection of these diagrams. For example, reaction of coordinatively unsaturated metal dialkyls and hydrido alkyls with carbon monoxide will lead to the reductive elimination of alkanes rather than formation of ketones and aldehydes. The results of this work are compared to earlier ion cyclotron resonance studies of related reactions at thermal energies.

Introduction

Studies in our laboratory have provided detailed insights into the mechanism and energetics of reactions of atomic transition-metal ions with hydrocarbons.[2-6] These studies have utilized a specially designed ion beam apparatus that permits the relative kinetic energy to be varied over a wide range, making it possible to characterize not only exo-

---

† Contribution No. 6812.

[1] Present address: (a) Department of Chemistry, Yale University, New Haven, CT 06520. (b) Department of Chemistry, University of California, Berkeley, CA 94720.

[2] Armentrout, P. B.; Beauchamp, J. L. *J. Am. Chem. Soc.* **1981**, *103*, 784.

0276-7333/84/2303-1694$01.50/0 © 1984 American Chemical Society

Table I. Product Distributions for Reactions of M^+ with Aldehydes and Ketones

		neutral products (irrespective of label)[a,b]												
neutral reactant	M^+	CO	H_2	CH_4	C_2H_6	C_3H_8	C_4H_{10}	C_2H_4	C_4H_8	C_2H_4O	H_2 + C_2H_4O	C_3H_6O	H_2 + C_3H_6O	MH
H_2CO	Co^+		1.0											
CH_3CHO	Co^+			1.0										
	Fe^+			1.0										
$(CH_3)_2CO$	Co^+	0.10			0.90									
	Ni^+	0.12			0.88									
$(CD_3)_2CO$	Co^+	0.10			0.90									
	Fe^+	0.07			0.93									
	Ni^+	0.06			0.94									
$CH_3CH_2COCH_3$	Co^+		0.07	0.18		0.10		0.49		0.15				
$CH_3CD_2COCD_3$	Co^+ [c]		tr	0.19		0.08		0.61		0.12				
	Fe^+		0.30	0.15		0.10		0.38		0.07				
$(C_2H_5)_2CO$	Co^+		0.05		0.08		0.04	0.70				0.12		
	Fe^+ [d]		0.29		0.15[d]			0.26[d]				0.15[d]		
$(CH_3CD_2)_2CO$	Co^+		0.04		0.04		0.03	0.74				0.10		
$(CH_3)_3CCOCH_3$	Co^+			0.88					0.01	0.07	0.01			0.04
	Fe^+			1.0										
$(CH_3)_3CCH_2COCH_3$	Co^+			0.76					0.06	0.13		0.03	0.02[e]	0.02[e]

[a] The data from the reactions of labeled compounds were used to determine product ratios for the unlabeled reactants when two products coincided at the same mass. See text for discussion of structure of the neutral products. [b] The data for Fe^+ are taken from ICR studies of ref 9. All other product distributions listed are from ion beam reactions measured at ~0.5-eV relative kinetic energy. [c] The small amount of dehydrogenation seems to be an anomaly here. At 1-eV relative kinetic energy, dehydrogenation accounts for 9% of the reaction with 2-butanone and 7% for 2-butanone-α-d_5. [d] Because the reaction of Fe^+ with 3-pentanone-α,α′-d_4 was not performed, one cannot distinguish between loss of C_2H_6 and H_2CO, C_2H_4 and CO, and C_3H_6O and C_4H_{10}. The sum of this product distribution from ref 2 adds up to 85% of the total reaction. [e] These products have the same mass and cannot be distinguished from each other in this reaction.

thermic reactions but also endothermic and "high-energy" processes as well. Ancillary information is provided by ion cyclotron resonance (ICR) studies.[6] In the present work we employ these experimental methods to examine the reactions of first-row group 8 atomic transition-metal ions, mainly Co^+, with organic molecules containing the carbonyl group as a structural moiety.

There have been several recent studies of the gas-phase reactions of metal ions with aldehydes and ketones.[7-12] Corderman and Beauchamp[7] first reported ICR studies of the decarbonylation (e.g., reaction 1) of acetaldehyde by

$$CpNi^+ + CH_3CHO \rightarrow CpNi(CO)^+ + CH_4 \qquad (1)$$

$CpNi^+$ (Cp ≡ η^5-C_5H_5). Interestingly, this species was unreactive with acetone and formaldehyde. Using ICR techniques, Freiser and co-workers have examined the reactions of Cu^+ and Fe^+ with ketones.[8,9] While copper ions either dehydrate ketones or cleave them into an enol (or ketone) and alkene, Fe^+ exhibits a richer variety of reactions.[9] These include dehydrogenation and decarbonylation processes, along with generation of alkenes, alkanes, and smaller ketones. Kappes and Staley[11] as well as Ridge[12] and co-workers have also examined reactions of atomic transition-metal ions with a range of cyclic and acyclic ketones.

In this paper we report detailed studies of the reactions of Co^+ with acetone, acetaldehyde, and formaldehyde, using the variable kinetic energy in the ion beam experiment as an important parameter to probe the mechanism and energetics of processes analogous to reaction 1. Less extensive results are presented for more complex cyclic and acyclic ketones. Deuterium labeling is employed to provide additional mechanistic information.

Experimental Section

The ion beam apparatus and experimental techniques have been described in detail.[2] Briefly, singly charged cobalt ions are formed by thermal dissociation and surface ionization of $CoCl_2 \cdot 6H_2O$ on a heated rhenium ribbon. The metal ions are mass selected and decelerated to the desired energy before entering a collision chamber containing the reactant gas. Product ions scattered in the forward direction are focused into a quadrupole mass filter and detected by using a channeltron electron multiplier operated in a pulse-counting mode.

All unlabeled samples were commercially available. Deuterated acetone was obtained from Stohler Isotope Chemicals (99.5 atom % D). Labeled 2-butanone and 3-pentanone were obtained by repetitive exchange with D_2O (99.8 atom % D) in the presence of small amounts of NaOD.[13] The ketones were separated from the aqueous phase by ether extractions that were dried with anhydrous $MgSO_4$. The ether was distilled off, with a final separation made by gas chromatography. Mass spectrometric analysis indicated preparation of 2-butanone-α,α′-d_5 with 98.0 atom % D and 3-pentanone-α,α′-d_4 with 97.5 atom % D. NMR analysis performed for the 3-pentanone confirmed selective deuteration at the α-position. Another sample of the labeled 2-butanone (98%) was obtained from Kor Isotopes. Cyclopentanone-α,α′-d_4 was prepared by adding 25 mL of D_2O and 2 drops of NaOD to 1 mL of cyclopentanone. The mixture was stirred under reflux at 70 °C for 24 h. As with the ketones described above, cyclopentanone was extracted with ether and dried over $MgSO_4$. The ether was distilled off with a final separation by GC. Mass spectrometric analysis indicated labeling to an extent of 96 atom % D.

---

(3) Halle, L. F.; Armentrout, P. B.; Beauchamp, J. L. *Organometallics* **1982**, *1*, 963.

(4) Armentrout, P. B.; Halle, L. F.; Beauchamp, J. L. *J. Am. Chem. Soc.* **1981**, *103*, 6624.

(5) Armentrout, P. B.; Beauchamp, J. L. *J. Am. Chem. Soc.* **1981**, *103*, 6628.

(6) Halle, L. F.; Houriet, R.; Kappes, M. M.; Staley, R. H.; Beauchamp, J. L. *J. Am. Chem. Soc.* **1982**, *104*, 6293.

(7) Corderman, R. R.; Beauchamp, J. L. *J. Am. Chem. Soc.* **1976**, *98*, 5700.

(8) Burnier, R. C.; Byrd, G. D.; Freiser, B. S. *Anal. Chem.* **1980**, *52*, 1641.

(9) Burnier, R. C.; Byrd, G. D.; Freiser, B. S. *J. Am. Chem. Soc.* **1981**, *103*, 4360.

(10) (a) Jacobson, D. B.; Freiser, B. S. *J. Am. Chem. Soc.* **1983**, *105*, 736. (b) Jacobson, D. B.; Freiser, B. S. *Ibid.* **1983**, *105*, 5197.

(11) Kappes, M. M. Ph.D. Thesis, Massachusetts Institute of Technology, 1981.

(12) Ridge, D. P.; Allison, J. "Twenty Sixth Annual Conference on Mass Spectrometry and Allied Topics", 1978, p 224.

(13) Caserio, M. C.; Beauchamp, J. L. *J. Am. Chem. Soc.* **1972**, *94*, 2638.

Table II. Product Distributions for the Reactions of M^+ with Cyclopentanone

neutral reactant	M^+	neutral products (irrespective of label)				
		CO^a	H_2	$C_4H_8{}^b$	$H_2 + CO^c$	$CO + C_2H_4$
cyclopentanone	$Co^{+\,d,e}$	0.44		0.02	0.52	0.02
	$Fe^{+\,f}$	0.30	0.11	0.10	0.49	
	$Co^{+\,f,g}$	0.08	0.05	0.05	0.82	
	$Ni^{+\,f}$	0.39		0.13	0.48	
	$Ni^{+\,h}$	0.50		0.17	0.33	
cyclopentanone-α,α'-d_4	$Co^{+\,d}$	0.50		0.02	0.46	0.02

[a] See ref 39. [b] This product cannot be distinguished from loss of $CO + C_2H_4$. (With the labeled compound, a peak of 87 amu appeared, attributed to loss of $C_4H_4D_4$ in this table, but it could be due to loss of $CO + C_2D_4$.) [c] The neutral product may be H_2CO. [d] Product distributions measured at 0.6-eV relative kinetic energy using the ion beam apparatus. [e] Data from reactions of the labeled compound were used to determine branching ratios in the reactions with the unlabeled reactants when two products coincided at the same mass. See footnote *b* of this table. [f] Data taken from ICR studies of ref 10. [g] See ref 40. [h] Data taken from ICR studies of ref 6.

Table III. Distribution of Labeled Products in the Reactions of M^+ with Labeled Ketones[a,b]

natural reactant		HD	CHD_3	$C_2H_4D_2$	C_2D_6	$C_3H_3D_5$	$C_4H_6D_4$	C_2H_3D	$C_2H_2D_2$	C_2HD_3O	C_2D_4O	$C_3H_4D_2O$	$C_3H_3D_3O$
$(CD_3)_2CO$	Co^+				1.0								
$CH_3CD_2COCD_3$	Co^+	1.0	1.0			1.0		0.19	0.81	0.79	0.21		
	Fe^+	1.0	1.0			1.0			1.0	1.0			
$(CH_3CD_2)_2CO$	Co^+	1.0		1.0			1.0	0.12	0.88			0.86	0.14

[a] Distributions for Co^+ reactions measured in ion beam at ~0.5 eV relative kinetic energy. Data for Fe^+ taken from ICR studies of ref 9. [b] See text for discussion of structure of the neutral products.

Table IV. Distribution of Label for Reaction of Co^+ with Cyclopentanone-α,α'-d_4 To Yield $Co[C_4(H,D)_6]^+ + (H,D)_2 + CO^a$

product	fractional yield
H_2	0.48
HD	0.35
D_2	0.17

[a] Measured at 0.6-eV relative kinetic energy.

Reaction cross sections for specific products, σ_i, are obtained by using eq 2 and 3, which relate the total cross section, σ, the

$$\sigma = \ln\,[(I_0 + \textstyle\sum I_i)/I_0]/n_0 l \qquad (2)$$

$$\sigma_i = \sigma I_i/\textstyle\sum I_i \qquad (3)$$

number density of the target gas, n_0, and the length of the colision chamber, l (5 mm), to the transmitted reactant ion beam intensity, I_0, and the sum of the product ion intensities, $\sum I_i$. Except as noted, the pressure of the target gas, measured by using an MKS Baratron Model 90H1 capacitance manometer, is kept low, usually $<1 \times 10^{-3}$ torr. It has been previously noted that cross sections for reactions with heavier hydrocarbons were not accurately reproducible,[2] presumably due to substantial loss of elastically scattered Co^+ from the reactant beam. Branching ratios were found to be reproducible, and the results for the larger ketones are reported in this manner.

Results and Discussion

The product distributions for the reactions of cobalt ions with several aldehydes and ketones are listed in Tables I through IV. We consider first the series $(CH_3)_2CO$, CH_3CHO, and H_2CO, where methyl groups are sequentially replaced with hydrogen atoms.

Acetone. Data for the reaction of Co^+ with acetone are shown in Figure 1. Cross sections for processes 4 and 5 are large at low energies and decrease with increasing energy, indicating that both reactions are exothermic. The identities of these products were checked by using CD_3COCD_3 (Table III).

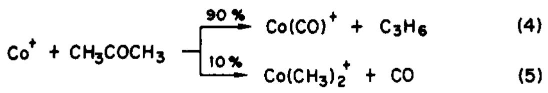
$$Co^+ + CH_3COCH_3 \begin{cases} \xrightarrow{90\%} Co(CO)^+ + C_3H_6 & (4) \\ \xrightarrow{10\%} Co(CH_3)_2^+ + CO & (5) \end{cases}$$

Also seen at low energies is the Co^+–acetone adduct, with the diadduct appearing at higher pressures. A log–log plot of $\sigma_i p$ (eq 2) vs. p, where p is the pressure of the target gas, is shown in Figure 2 for the major products at a relative kinetic energy of 1 eV. The slopes of the lines for $Co(CO)^+$ and $Co(CH_3)_2{}^+$ are 0.99 and 1.18, respectively, which are close to the value expected for a purely bimolecular process (i.e., the cross sections for production of these species are independent of pressure). The slope for the cobalt ion–acetone adduct in Figure 2 is 1.86, indicating a termolecular process. This product may result either from collisional stabilization of the reaction intermediate in processes 4 and 5 or by further reaction of the products of these reactions with acetone (ligand displacement processes). Although the data are limited, the slope for the diadduct in Figure 2 suggests an even higher order process.

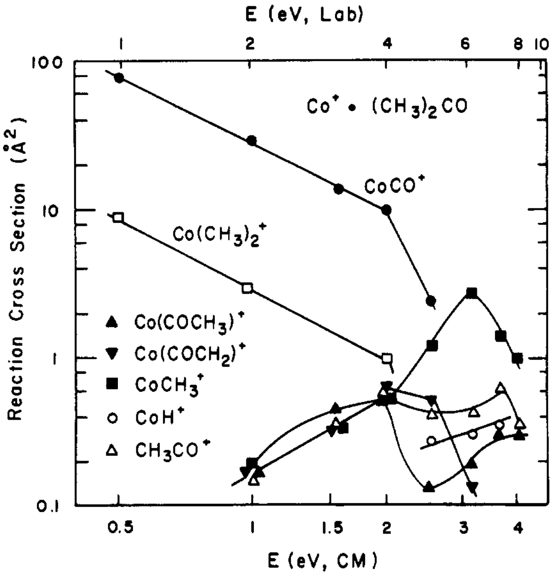

Figure 1. Variation in reaction cross section for the interaction of Co^+ with acetone as a function of kinetic energy in the center of mass frame (lower scale) and laboratory frame (upper scale).

The low-energy products can be accounted for by the steps depicted in Scheme I. The general reaction coordinate diagram is shown in Figure 3. Cobalt ions insert into the C–CO bond of acetone, followed by a methyl migration onto the metal center to form 2. This type of methyl shift has many precedents in the literature.[14]

Scheme I

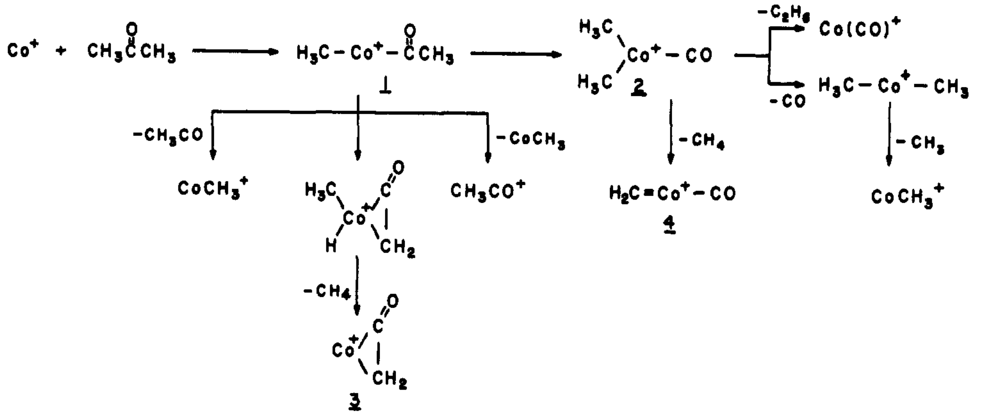

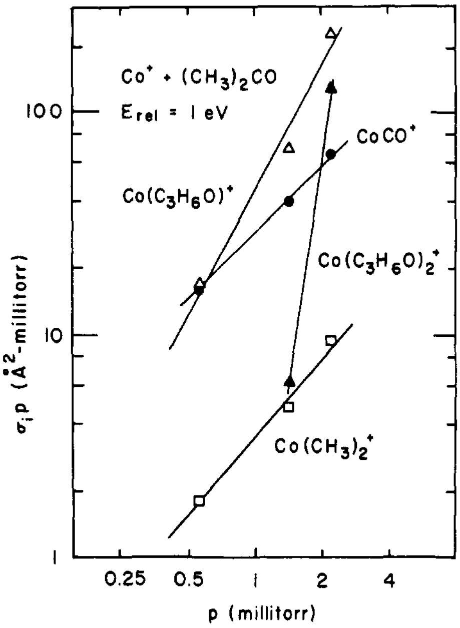

Figure 2. Plot of the product of the reaction cross section and pressure, $\sigma_i p$, vs. pressure for the major products of the reaction of Co^+ with acetone at 1 eV relative kinetic energy. The slopes of the lines drawn are 0.99 [$CoCO^+$], 1.18 [$Co(CH_3)_2{}^+$], 1.86 [$Co(C_3H_6O)^+$], and 6.73 [$Co(C_3H_6O)_2{}^+$].

Intermediate 2 can either reductively eliminate ethane, resulting in formation of the major product $Co(CO)^+$ or lose CO to give the dimethyl species $(CH_3)_2Co^+$. The decomposition of acetone into CO and two methyl radicals requires 96 kcal/mol[15,16] (Table V). Thus, the exothermic production of $(CH_3)_2Co^+$ indicates that the sum of the two methyl bond dissociation energies to Co^+ exceeds this amount. This same limit applies to the ions $(CH_3)_2Fe^+$[9] and $(CH_3)_2Ni^+$,[17] formed in the analogous exothermic reactions of Fe^+ and Ni^+ with acetone (Table I). These results confirm an earlier contention that processes involving insertion of first-row group 8 metal ions into C–C bonds of alkanes are exothermic.[2,3,18]

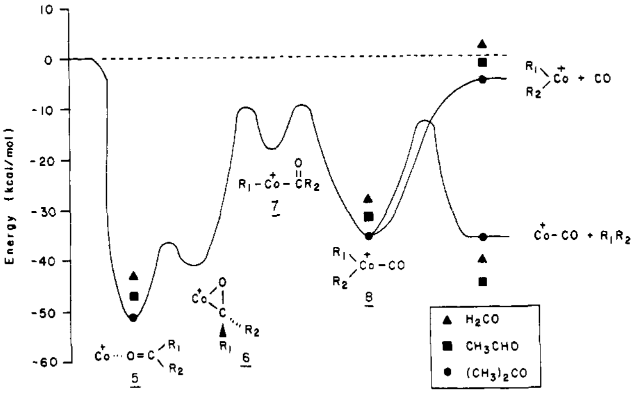

Figure 3. Simplified reaction coordinate diagram for the interaction of Co^+ with acetone (●), acetaldehyde (■), and formaldehyde (▲). The curve is drawn through the points calculated for the acetone reaction.

Table V. Reaction Enthalpies Used in Text

	ΔH,[a] kcal/mol
$H_2CO \rightarrow HCO + H$	87
$\rightarrow CO + 2H$	103.7
$\rightarrow CO + H_2$	-0.3
$CH_3CHO \rightarrow CH_3CO + H$	86.0
$\rightarrow HCO + CH_3$	82.5
$\rightarrow CO + H + CH_3$	100.5
$\rightarrow CO + CH_4$	-4.6
$(CH_3)_2CO \rightarrow CH_3CO + CH_3$	81.2
$\rightarrow CO + 2CH_3$	95.7
$\rightarrow CO + C_2H_6$	5.3
$\rightarrow CO + H_2 + C_2H_4$	38.0
$\rightarrow CH_3COCH_2 + H$	98.3
$CH_3COC_2H_5 \rightarrow CH_3CO + C_2H_5$	77.1
$\rightarrow C_2H_5CO + CH_3$	80.6
$\rightarrow CO + CH_3 + C_2H_5$	91.6
$\rightarrow CO + C_3H_8$	5.8
$\rightarrow CO + CH_4 + C_2H_4$	25.2
$\rightarrow COCH_3 + C_2H_4 + H$	115.8
$\rightarrow HCOCH_3 + C_2H_4$	29.8
$\rightarrow CH_3COCH_2 + CH_3$	75.4
$(C_2H_5)_2CO \rightarrow COC_2H_5 + C_2H_5$	77.4
$\rightarrow CO + 2C_2H_5$	87.0
$\rightarrow CO + C_4H_{10}$	4.9
$\rightarrow CO + C_2H_4 + C_2H_6$	27.4
$\rightarrow COC_2H_5 + C_2H_4 + H$	116.0
$\rightarrow HCOC_2H_5 + C_2H_4$	28.6
$\rightarrow CH_2COC_2H_5 + CH_3$	86.4

[a] From ref 15 and 16.

At higher energies reactions 6–9 are observed. Observation of energy thresholds for these processes indicates that they are endothermic reactions or have fairly high activation energies. The second of these has a maximum

---

(14) Kuhlman, E. J.; Alexander, J. J. *Coord. Chem. Rev.* **1980**, *33*, 195. Flood, T. C.; Jenson, J. E.; Statler, J. A. *J. Am. Chem. Soc.* **1981**, *103*, 4410. Migratory insertion processes have also been noted in cationic iron systems: Magnuson, R. H.; Zulu, S.; T'sai, W.-M.; Giering, W. P. *J. Am. Chem. Soc.* **1980**, *102*, 6888.

(15) Supplementary heats of formation of organic molecules are taken from: Cox, J. D.; Pilcher, G. "Thermochemistry of Organic and Organometallic Compounds"; Academic Press: New York, 1970.

(16) Heats of formation of organic radical species are taken from: McMillen, D. F.; Golden, D. M. *Annu. Rev. Phys. Chem.* **1982**, *33*, 493.

(17) Halle, L. F.; Beauchamp, J. L., unpublished results.

(18) Carbon–carbon bond dissociation energies of alkanes are typically in the range of 70–90 kcal/mol.[16]

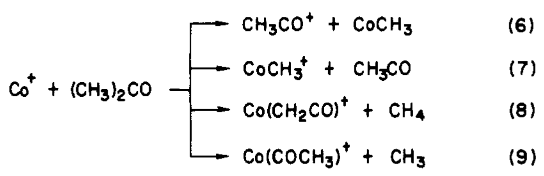

$$Co^+ + (CH_3)_2CO \rightarrow CH_3CO^+ + CoCH_3 \quad (6)$$
$$\rightarrow CoCH_3^+ + CH_3CO \quad (7)$$
$$\rightarrow Co(CH_2CO)^+ + CH_4 \quad (8)$$
$$\rightarrow Co(COCH_3)^+ + CH_3 \quad (9)$$

cross section of 3 Å^2 at 3.1 eV. The remainder are minor products, with maximum cross sections less than 1 Å^2. All four have thresholds between 0.5 and 1.0 eV. It is difficult to say which process has the lowest threshold. The endothermic reactions 6–9 of Co^+ with acetone provide additional clues as to the nature of reaction intermediates involved in the formation of $CoCO^+$ and $Co(CH_3)_2{}^+$ at low energy. For example, simple cleavage of the metal–acyl bond in 1 would yield the products of reactions 6 and 7. These reactions dominate at higher energies due to their favorable frequency factors.[19] Thresholds and product ion abundances for both processes are comparable, indicating that the ionization energies of CH_3Co and CH_3CO are similar. Earlier estimates give the ionization potential of $CoCH_3$, IP[$CoCH_3$], in the range of 6.70–7.36 eV,[2] to be compared with IP[CH_3CO] = 7.04 eV.[16,20] Pyrolysis of acetone yields ketene and methane (reaction 10),[21] a process

$$(CH_3)_2CO \rightarrow CH_2CO + CH_4 \qquad (10)$$

cess which is endothermic by 20 kcal/mol.[15] The binding energy of ketene to Co^+ is very likely in excess of this amount (see Appendix), rendering the overall process exothermic. The data in Figure 1 indicate that reaction 8 requires excess energy to be observed, suggesting that the process has a moderate activation energy. Possible structures for the product are indicated by 3 and 4. The extent of σ bonding in 3 (which may also be represented as a π complex) is not known. Our estimates (see Appendix) suggest that 3 and 4 have comparable stabilities.[22] Plausible mechanisms leading to 3 and 4 involve β-hydrogen transfer starting from 1 and elimination of CH_4 from 2, respectively. Apparently, these processes have frequency factors or activation energies that do not allow them to compete with the major pathways except at high interval energies.

Reaction 9 is interesting since this product might result from cleavage of the metal–methyl bond in either 1 or 2. Thermochemical estimates (see Appendix) indicate that $(CH_3)CoCO^+$ is more stable than $Co(COCH_3)^+$ by ~20 kcal/mol (i.e., methyl migration from the carbonyl to the metal is exothermic). Hence, the metal–methyl bond in 2 can be cleaved at a lower energy than in 1. It is possible that both processes are occurring, giving rise to the unusual structure in the cross section shown for this process in Figure 1.

The semiquantitative potential energy diagram shown in Figure 3 is useful for further discussing the reactions of Co^+ with acetone. Thermochemical data used to construct this diagram are discussed in detail in the Appendix. The initial interaction generates a chemically activated species, 5, with an internal energy approximately equal to the binding energy of acetone to Co^+ (51 kcal/mol). This species may have either a linear geometry with respect to the carbonyl group, which is characteristic of an electrostatic interaction (e.g., with Li^{+}[23]) or a bent structure such as 9 depending on the degree of covalent bonding. The precursor to the methyl shift onto the metal is probably 6, with η^2-bound acetone. Although we think the linear structure is more stable (see Appendix), the mode of bonding shown for acetone in 6 is characteristic of the binding of aldehydes and ketones to metals in coordinatively saturated complexes.[24]

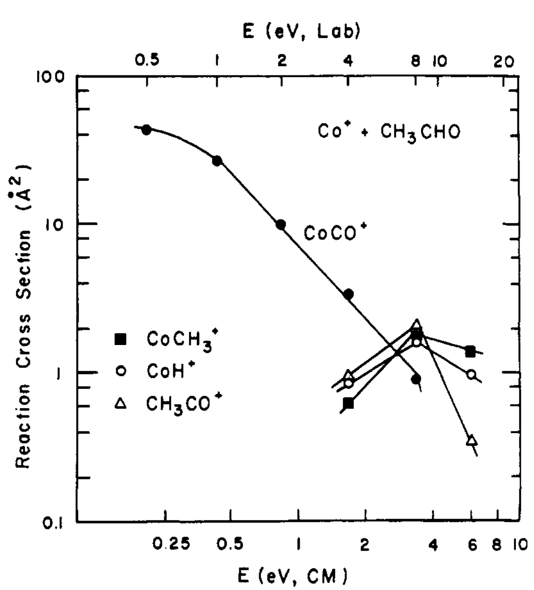

Figure 4. Variation in reaction cross section for the interaction of Co^+ with acetaldehyde as a function of kinetic energy in the center of mass frame (lower scale) and laboratory frame (upper scale).

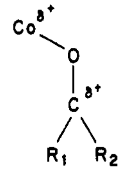

9

Rearrangement of 5 to allow interaction of Co^+ with the π system of the carbonyl group is followed by addition of the metal ion to one of the two C–C bonds of acetone, yielding 7. A methyl migration from CO to the metal forms 8, which can reductively eliminate ethane or lose CO. The minor product $Co(CH_3)_2{}^+$ is only slightly exothermic, while $Co(CO)^+$ is 35 kcal/mol exothermic. The activation energy for reductive elimination of ethane from 8 is expected to be high.[25] If this were not the case, $Co(CH_3)_2{}^+$ would not be formed competitively in the reaction of Co^+ with acetone. This barrier is also consistent with the observation that the reverse process, insertion of $Co(CO)^+$ into the carbon–carbon bond of an alkane to form a structure analogous to 7, has not been observed in limited studies of the reactions of $Co(CO)^+$ with several alkanes.[26] In contrast, bare cobalt ions readily add to carbon–carbon bonds of alkanes.[2] Loss of CO from 8, a simple bond

---

[19] Robinson, P. J.; Holbrook, K. A. "Unimolecular Reactions"; Wiley: London, 1972.

[20] Traeger, J. C.; McLoughlin, R. G.; Nicholson, A. J. C. *J. Am. Chem. Soc.* **1982**, *104*, 5318.

[21] Williams, J. W.; Hurd, C. D. *J. Org. Chem.* **1940**, *5*, 122.

[22] The fact that $CoCH_2{}^+$ is not observed as a prominent reaction product at higher energies may suggest that 3 is somewhat more stable.

[23] Woodin, R. L.; Houle, F. A.; Goddard, W. A., III *Chem. Phys.* **1976**, *14*, 461.

[24] (a) Brown, K. L.; Clark, G. R.; Headford, C. E. L.; Marsden, K.; Roper, W. R. *J. Am. Chem. Soc.* **1979**, *101*, 503. (b) Walther, D. J. *J. Organomet. Chem.* **1980**, *190*, 393. (c) Driessen, W. L.; Groeneveld, W. L. *Recl. Trav. Chem. Pays-Bas* **1969**, *88*, 1977.

[25] Activation energies for reductive elimination of ethane and methane from platinum complexes are discussed in: Brown, M. P.; Puddephatt, R. J.; Upton, C. E. E. *J. Chem. Soc., Dalton Trans.* **1974**, 2457. Abis, L.; Sen, A.; Halpern, J. *J. Am. Chem. Soc.* **1978**, *100*, 2915.

[26] Freas, R. B.; Ridge, D. P. *J. Am. Chem. Soc.* **1980**, *102*, 7129.

Scheme II

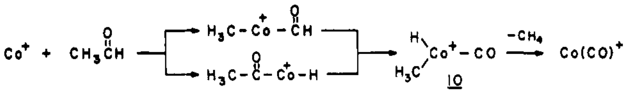

Table VI. Thermochemical Estimates Used in Constructing Reaction Coordinate Diagrams

bond	binding energy, kcal/mol
$Co^+\cdots O{=}CH_2$	43
$Co^+\cdots O{=}CHCH_3$	47
$Co^+\cdots O{=}C(CH_3)_2$	51
$Co^+\cdots$cyclopentanone	50
$Co^+\cdots(CH_2CO)$	>40
$Co^+{-}H$	52 ± 4[a]
$Co^+{-}CH_3$	61 ± 4[a]
$Co^+{=}CH_2$	85 ± 7[a]
$(H)Co^+{-}H$	50
$(H_3C)Co^+{-}H$	41
$(H_3C)Co^+{-}CH_3$	40
$Co^+{-}CO$	40
$RCo^+{-}CO$	35
$(R_1)(R_2)Co^+{-}CO$	30
$H_2C{=}Co^+{-}CO$	30
$Co^+{-}C(O)R$	60
$(H_3C)Co^+{-}C(O)R$	40
$HCo^+{-}C(O)R$	50
$Co^+{-}(C_2H_4)$	50
$(C_2H_4)Co^+{-}(C_2H_4)$	40
$Co^+{-}(C_4H_6)$	56

[a] Reference 30.

cleavage process, is not expected to have an activation energy much in excess of the endothermicity. The fact that the ratio of $Co(CH_3)_2^+$ to $CoCO^+$ remains relatively constant as a function of translational energy indicates that activation energies for processes 4 and 5 are comparable.

Acetaldehyde. The only product formed at low energies in the reaction of cobalt ions with acetaldehyde is $Co(CO)^+$ (process 11). The data for this reaction are

$$Co^+ + CH_3CHO \rightarrow Co(CO)^+ + CH_4 \qquad (11)$$

shown in Figure 4 and indicate that reaction 11 is an exothermic process. Adduct formation at the lowest energies is also prominent. At higher energies, endothermic formation of CH_3CO^+, CoH^+, and $CoCH_3^+$ occurs. A species corresponding to $Co(H)(CH_3)^+$ is not observed at any energy.

Scheme II shows a mechanism by which reaction 11 can occur. After an initial interaction with the carbonyl moiety, Co^+ inserts into the H–CO or C–CO bond of acetaldehyde. Methyl or hydrogen migration from CO onto the metal then precedes reductive elimination of CH_4. The absence of the $Co(H)(CH_3)^+$ species may indicate that the process is endothermic (this would be the case if D-$[HCo^+{-}CH_3]$ were less than 49 kcal/mol) or that the activation energy for the reductive elimination of methane from **10** is very low.[25] Thermochemical data in Table VI are chosen such that formation of $Co(H)(CH_3)^+$ is 2 kcal/mol exothermic, as shown in Figure 3.

We would like to be able to say whether Co^+ adds first to the C–CO or H–CO bond of acetaldehyde. With use of the thermochemical estimates given in the Appendix, there is little difference in the energy of **7** for R_1 = H, R_2 = CH_3 and R_1 = CH_3, R_2 = H. The above results for acetone indicate that cobalt ions do insert into the C–CO bond and that methyl migration from CO to the metal center can occur. Results discussed below for formaldehyde suggest that either addition of Co^+ to the H–CO bond or the subsequent hydrogen transfer is a difficult process. At higher energies, insertion of Co^+ into both the C–CO and H–CO bond is suggested by observation of the endothermic products $CoCH_3^+$ and CoH^+. On the basis of the value IP(CoH) = 7.3 ± 0.1 eV[2], formation of CoH^+ should require only ~5 kcal/mol more energy than $COCH_3^+$.[16,20] At 1.7-eV relative kinetic energy, slightly above threshold, comparable amounts of these two products are observed. The appearance of HCO^+ was not examined.

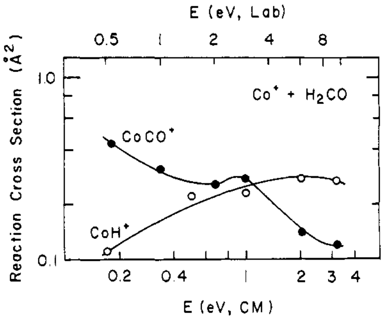

Figure 5. Variation in reaction cross section for the interaction of Co^+ with formaldehyde as a function of kinetic energy in the center of mass frame (lower scale) and laboratory frame (upper scale).

Formaldehyde. Cobalt ions react with formaldehyde to form $Co(CO)^+$ (eq 12). Data for this reaction are shown

$$Co^+ + H_2CO \rightarrow Co(CO)^+ + H_2 \qquad (12)$$

in Figure 5. Surprisingly, unlike the results for the $Co(CO)^+$ ion formed in reactions 4 and 11, the cross section for reaction 12 is very small at low energies (<1 Å²) and decreases slowly with energy. A small amount of CoH^+ is seen at low energies, but the cross section for this product increases with increasing energy, suggesting an endothermic process. The dihydrido species $Co(H)_2^+$ is not observed at any energy examined.

The decarbonylation processes seen in these gas-phase reactions have their parallels in condensed-phase studies. For example, certain rhodium[27] and osmium[28] complexes are known to react with acetaldehyde to form the metal hydrido acyl compound. Upon heating, the hydrido acyl undergoes migratory deinsertion followed by reductive elimination to yield the metal carbonyl complex and an alkane. Similarly, hydrido formyl complexes of Ir(III)[29] and Os(0)[24a] have been prepared by the direct oxidative addition of the C–H bond of formaldehyde. Formation of the hydrido formyl is probably preceded by formation of a complex containing a π-bound H_2CO entity, analogous to the chemically activated species **6**.[24a] When heated, the hydrido formyl complexes decompose with one product of the decomposition being hydrogen gas.[24a]

It is not clear why decarbonylation of formaldehyde by gas-phase ions should be less facile than that of acetaldehyde or acetone. The energetics involved in the conversion of the organic substrates R_1COR_2, where R_1, R_2 = H or CH_3, to $R_1CO + R_2$ are given in Table V. Cleavage of the H–CO bond requires only ~5 kcal/mol more energy than cleavage of the H_3C–CO bond. With use of the thermochemical estimates from Table VI, Figure 3 places **7** at approximately the same energy relative to reactants for acetone, acetaldehyde, and formaldehyde.

Some distinctions can be made in comparing the present results to condensed-phase studies. The metal–carbon bond energies in organometallic fragment ions often exceed

---

(27) Milstein, D. *Organometallics* **1981**, *1*, 1549.

(28) Headford, C. E. L.; Roper, W. R. *J. Organomet. Chem.* **1980**, *98*, C7.

(29) Thorn, D. L. *Organometallics* **1982**, *1*, 197. Thorn, D. L. *J. Am. Chem. Soc.* **1980**, *102*, 7109.

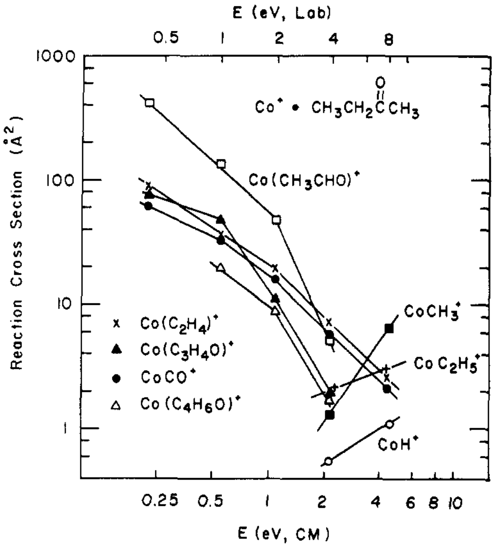

Figure 6. Variation in reaction cross section for the interaction of Co^+ with 2-butanone as a function of kinetic energy in the center of mass frame (lower scale) and laboratory frame (upper scale).

the analogous metal–hydrogen bond strengths because the polarizable methyl group stabilizes the charge more favorably than hydrogen.[30] This effect is diluted by additional polarizable ligands as well as by a dielectric medium. Thus metal–hydrogen bonds are expected to be stronger than metal–carbon bonds in solvated complexes or those with more ligands attached. Hence, unsolvated bare metal ions may be uniquely suited as reagents for decarbonylation of ketones.

Interestingly, reactions of Ni^+ and Rh^+ with formaldehyde yield $M(CO)^+$ as the only product ion at low energies, again with a very small cross section.[17] The reactions of Ni^+ might be expected to be similar to Co^+, given the similar types of products observed in the reactions of the three first-row group 8 metal ions with alkanes.[3] However, at low energies Rh^+ exclusively dehydrogenates alkanes, including ethane.[31] Because of this selectivity toward C–H bond insertion in alkanes, one might expect a greater reactivity toward the C–H bonds of formaldehyde. This does not occur.

The small cross sections for reactions of metal ions with formaldehyde in the gas phase may have less to do with overall thermochemistry than with the relative magnitude of reaction and dissociation rates for the initially formed adduct **5**. Little of the adduct is seen in the formaldehyde reactions, while it is quite prominent at low energies in the acetone and acetaldehyde reactions.

The rate of dissociation of the chemically activated intermediate **5** to regenerate the reactants varies considerably with the number of vibrational degrees of freedom in the adduct. More importantly, an RRKM analysis indicates the ratio of unimolecular reaction to dissociation at a given level of internal energy increases with increasing substitution of CH_3 for H. With formaldehyde it is possible that dissociation is significantly faster than the initial rearrangement step leading to decarbonylation.[32]

Scheme III

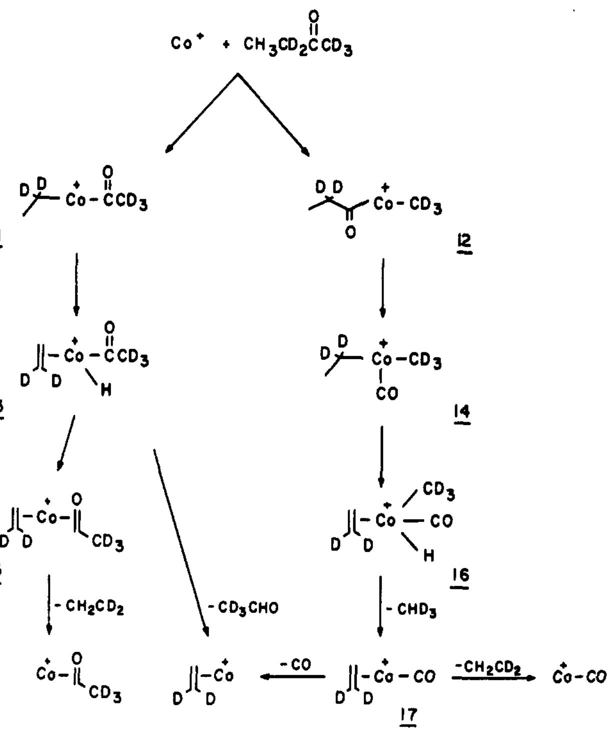

Larger Dialkyl Ketones. Once the ketone has a longer alkyl chain, a greater variety of products appears. For example, Figure 6 depicts the data for the reaction of Co^+ with 2-butanone. Butanone-α,α'-d_5 was used to identify the products listed in Table I. A number of pathways can lead to the same product as shown in Scheme III. The initial insertion product can be to either of the C–CO bonds of the ketone. If insertion occurs into the $OC–C_2H_5$ bond, a β-hydrogen can be transferred to the metal to form **13**. Structure **13** can lose ethene or rearrange further to **15**, which can lose either ethene or acetaldehyde. Alternatively, structure **16** may be generated if insertion into either C–CO bond is followed by an alkyl migration onto the metal center. This intermediate may be a common precursor to all product ions. Losses of methane, ethene, and carbon monoxide can follow. Because ethene is more strongly bound to metal cations than CO,[33] structure **16** would be expected to lose more CO than ethene. However, no $Co(C_3H_3D_5)^+$ is observed. This suggests that loss of CHD_3 precedes loss of ethene and loss of CO from **16**. Likewise, because the binding energy of acetaldehyde to Co^+ is expected to be much greater than that of ethene, intermediate **15** most likely loses only ethene.[7] This leaves **13** or **17** as the likely precursors to the Co(ethene)$^+$ product. The species corresponding to $Co(C_2HD_3O)^+$ is expected to be a cobalt ion bound to acetaldehyde. Exothermic formation of $Co(H)(COCD_3)^+$ from butanone would imply that $D[HCo^+–COCD_3] > 63$ kcal/mol (Tables V and VI). If this were the case, the $Co(COCH_3)^+$ species should appear at much lower energies ($\sim$0.5 eV) than it does in the reaction of Co^+ with acetone.

In contrast to the reaction with acetone, simple loss of CO is not observed. This may suggest that alkyl migration from CO onto the metal ion is slow compared to β-hydrogen transfers; i.e., **13** is formed more rapidly than **14**. Another possibility, although unlikely, is that formation of $Co(CH_3)(C_2H_5)^+$ from reaction with butanone is endothermic. This would result if the sum of the two metal–

---

[30] Armentrout, P. B.; Halle, L. F.; Beauchamp, J. L. *J. Am. Chem. Soc.* **1981**, *103*, 6501.

[31] Byrd, G. D.; Freiser, B. S. *J. Am. Chem. Soc.* **1982**, *104*, 5944.

[32] The reactions of these bare metal ions can be compared to the 14-electron cyclopentadienyl nickel ion $CpNi^+$. $CpNi^+$ is unreactive with both ethane and formaldehyde but, like Rh^+, does exclusively dehydrogenate larger alkanes.[7] However, because $CpNi^+$ has added vibrational degrees of freedom compared to the bare metal ion, the above argument concerning the lifetimes of the intermediate **5** is not as relevant. It has been suggested that $CpNi^+$ reacts by first abstracting H^- (Corderman, R. R. Ph.D. Thesis, California Institute of Technology, 1977).

[33] Ethene-d_4 is observed to displace CO from $Ni(CO)^{+6}$ and $Fe(CO)^+$; Foster, M. S.; Beauchamp, J. L. *J. Am. Chem. Soc.* **1975**, *97*, 4808.

Scheme IV

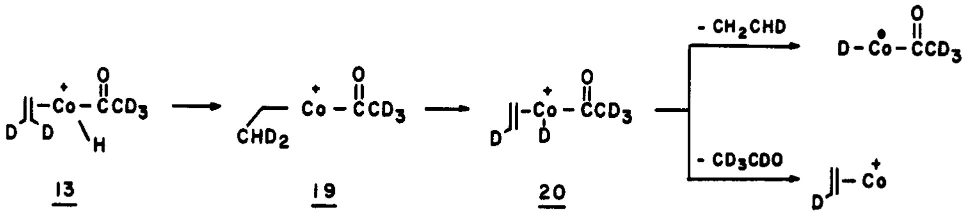

Scheme V

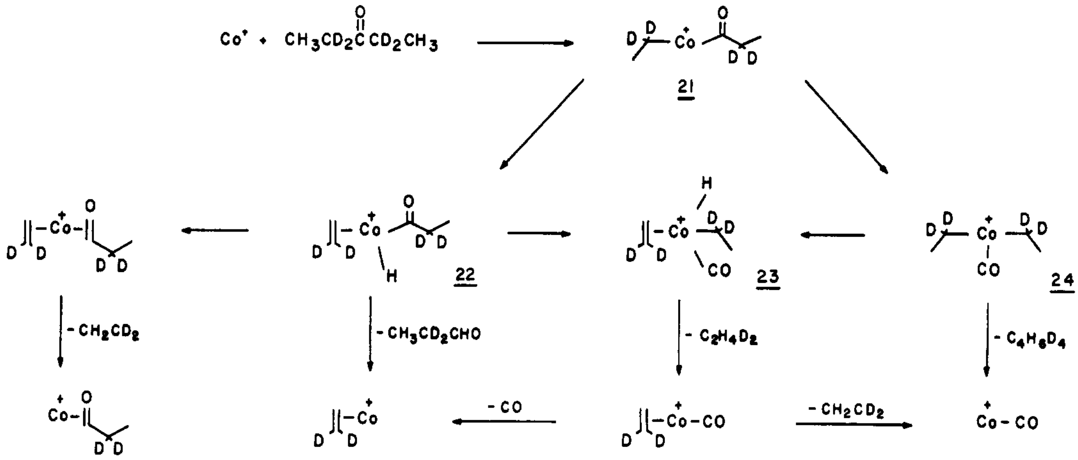

carbon energies were less than 92 kcal/mol.[15,16]

Reaction of Co^+ with butanone may also proceed via initial insertion into other bonds of the ketone. A small amount of dehydrogenation that occurs exclusively via loss of HD from the butanone-α,α'-d_5 is observed. Dehydrogenation most likely proceeds via insertion of the metal into the C–H or C–D bond of the ethyl group followed by β-D(H) transfer and loss of HD. The resulting ionic product is stabilized by a conjugated π system to which the metal can bind, structure **18**.[34]

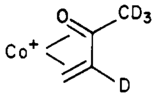

18

The major loss of CH_2CD_2 (81%) from the 2-butanone-α,α'-d_5 is rationalized as indicated in Scheme III. At the lowest energies, loss of C_2H_3D appears as well. The proportion of the latter decreases with increasing energy. This product is probably formed via a scrambling process. Scheme IV shows how this scrambling can occur once intermediate **13** is formed (Scheme III). The hydrogen that has been transferred onto the metal may be reversibly transferred back onto either end of the alkene. If it returns to the deuterated carbon, intermediate **19** is formed. This ion can undergo a β-D transfer to form **20**. Now either C_2H_3D or acetaldehyde-d_4 can be eliminated. Both of these products are observed. The analogous scrambling mechanism can in principle proceed via **16**, leading to loss of CD_4 as well. This may occur, though it is difficult to ascertain from our data. It is of interest to note that pathways similar to those depicted in Scheme IV appear to play a significant role in the low-energy reactions of Co^+ with alkanes.[2,35]

Products appearing at higher energies include $CH_3CD_2^+$, CD_3CO^+, $COCD_2CH_3^+$, $CoCD_3^+$, $Co(CD_2CH_3)^+$, $Co(COCD_3)^+$, and $Co(COCD_2CH_3)^+$. These may be formed by dissociation of intermediates **11** and **12** by simple cleavage of the Co^+–carbon bonds. The $CoCH_3^+$ and $Co(CD_2COCD_3)^+$ ions are also observed at higher energies[36] and are probably the result of a process involving initial insertion into the C3–C4 bond. The cross section for the $CoCD_3^+$ ion is slightly greater than that for $CoCH_3^+$ at the energies where these products first appear. This is consistent with the slightly lower OC–CD_3 bond energy (Table V). These two cobalt–methyl ions account for >50% of the product distribution at 8 eV, the highest relative kinetic energy examined. In addition to the fragmentation of insertion intermediates, high-energy products may also result from direct (e.g., stripping) reactions.

Insertion into both C–H and C–D bonds takes place. The ratio of CoH^+ to CoD^+ is roughly 1:1 at relative kinetic energies from 1 eV ($\sigma_H \approx 0.3$ Å^2) to 8 eV ($\sigma_H \approx 1.1$ Å^2). Because the ratio of H:D in the labeled butanone is 3:5, the equivalent amounts of CoH^+:CoD^+ may indicate a favoring of C–H bond insertion over C-D bond insertion. However, this trend does not continue in the 3-pentanone-α,α'-d_4 discussed below.

Products observed in the reaction of Co^+ with 3-pentanone are listed in Table I. The products formed at low energies can be explained as indicated in Scheme V, which depicts processes similar to those in Scheme III. Cobalt ions add first to a C–CO bond of the ketone. β-Hydrogen abstraction off the ethyl group leads to **22**, or ethyl migration to the metal yields **24**. Loss of propanal or ethene from **22**, loss of butane from **24**, and loss of ethane from **23** lead to most products observed at low energies. As is the case in the butanone reaction, the $Co(C_3H_3D_2O)^+$ ion is expected to be a cobalt ion bound to an aldehyde, in this case propanal, rather than a hydrido acyl. Exothermic production of the latter would imply $D[HCo^+–COC_2H_5]$

---

[34] Also observed in the reactions of 2-butanone and 2-butanone-α,α'-d_5 is a small amount (3–6%) of $Co(COCH_2)^+$ that appears to be formed in an exothermic process. The generation of this product from the labeled butanone is difficult to explain.

[35] Houriet, R.; Halle, L. F.; Beauchamp, J. L. *Organometallics* **1983**, 2 1818.

[36] Hydridoacylmethyliridium compounds have also been generated in solution, see, for example: Milstein, D.; Calabrese, J. C. *J. Am. Chem. Soc.* **1982**, *104*, 3773.

Scheme VI

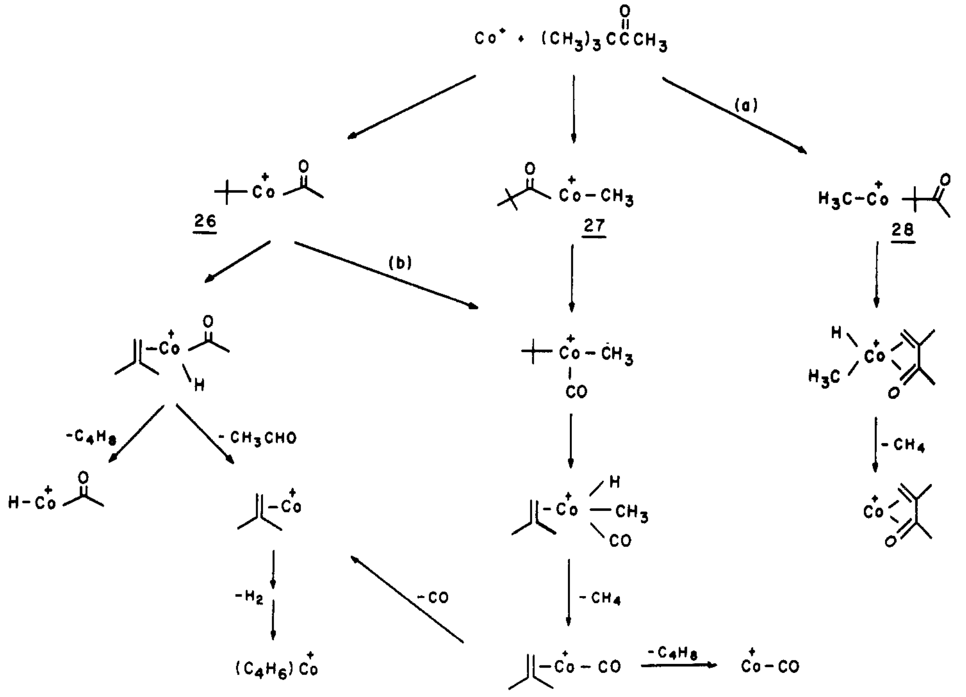

> 64 kcal/mol (Tables V and VI). This is unlikely for reasons discussed above.

A small amount of dehydrogenation, lost exclusively as HD from the 3-pentanone-α,α'-d_4, is also observed at low energies. In analogy to structure **18**, the dehydrogenation product is thought to be a cobalt ion bound to an α,β-unsaturated ketone, in this case, 1-penten-3-one. As in the case of 2-butanone-α,α'-d_5, a small amount (~2%) of $Co(CH_2CO)^+$ also appears as an exothermic process in the reaction with 3-pentanone-α,α'-d_4.[34]

Scrambling processes similar to those depicted in Scheme IV for 2-butanone-α,α'-d_5 are also apparent in the reactions of Co^+ with 3-pentanone-α,α'-d_4 (Table III). Analogous to Scheme IV, **22** can exchange the metal-bound hydrogen atom for one of the vinyl deuteriums, leading to loss of propanal-α,α'-d_3 or C_2H_3D. Because of the small amount of product due to loss of ethane, it could not be determined if scrambling processes occur during its formation as well.

At higher energies, Co^+ is seen to insert into all C–C and C–H bonds of the molecule. Simple cleavage products of intermediate **21**, $CD_2CH_3^+$, and $Co(CD_2CH_3)^+$ and of **25**, $CoCH_3^+$, and $Co(CH_3CD_2COCD_2)^+$ are observed. Some $Co(CD_2CO)^+$ appears at these high energies as well and is probably due to a complex rearrangement of **25**. The ratio of CoH^+:CoD^+ is ~1.2 from 1.2 to 20 eV in the center of mass frame, with a maximum cross section observed of ~1.7 Å^2. A statistical ratio accounting for the number of hydrogen to deuterium atoms would be 1.5.

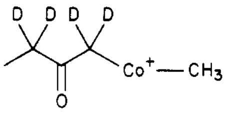

25

As the alkyl chain on the ketone becomes more complex, more of the product distribution is due to loss of an alkane. For example, 88% of the observed products in the reaction of Co^+ with 3,3-dimethyl-2-butanone are accounted for by loss of methane, and 76% loss of methane is observed in the reaction with 4,4-dimethylpentanone. Scheme VI depicts two pathways, a and b, through which methane can be lost from the dimethylbutanone. Both of these pathways have precedence in other reactions of cobalt ions. Path a is analogous to the proposed mechanism for loss of methane with 2,2-dimethylpropane.[2] The metal ion inserts into the terminal C–C bond, a β-hydrogen is transferred to the metal, and reductive elimination of CH_4 occurs. This can result in a cobalt ion bound to an α,β-unsaturated ketone. Alternatively, and consistent with Schemes III and V, Co^+ can enter the OC–C3 bond, followed by a methyl migration off the CO and a β-hydrogen transfer to the metal center, path b. In addition, processes similar to those depicted earlier with 2-butanone and 3-pentanone occur, such as loss of acetaldehyde and alkene (butene in this case). The cobalt–butene ion can further dehydrogenate by allylic hydrogen abstractions to form $Co(C_4H_6)^+$.[37] This product was also observed in the reaction of Co^+ with 2-methylpropene.[4] The structure of the $Co(C_4H_6)^+$ ion is uncertain. It may be a cobalt ion–trimethylenemethane complex. Other possibilities would result if substantial rearrangement is required before dehydrogenation occurs. High-energy products include cobalt–carbon cleavage products of **26**, **27**, and **28**, namely, CH_3CO^+, $C_4H_9^+$, $C_4H_9CO^+$, and $CoCH_3^+$. The CoH^+ ion is also observed.

Loss of methane from 4,4-dimethyl-2-pentanone can also be accounted for by two pathways. The first, shown in Scheme VIIa, is directly analogous to Scheme VIa. Here too, the product can be the metal ion bound to an α,β-unsaturated ketone. Another possible pathway is through Scheme VIIb. Intermediate **30** is formed from **29** via a β-methyl transfer to the metal. β-Methyl transfers have been noted in the reaction of Fe^+ with deuterated alkanes at low energies and also with Co^+ at slightly higher energies.[3,38] Intermediate **30** can lose either acetone or butene or abstract an allylic hydrogen from the 2-methylbutene to which it is bound.[4] Loss of methane or loss of acetaldehyde leading to **31** can then occur. This ion may

---

(37) The $C_7H_3O^+$ ion has the same mass as $Co(C_4H_6)^+$.

(38) β-Methyl transfers have been observed in condensed-phase reactions as well: Watson, P. L.; Roe, D. C. *J. Am. Chem. Soc.* **1982**, *104*, 6471.

Scheme VII

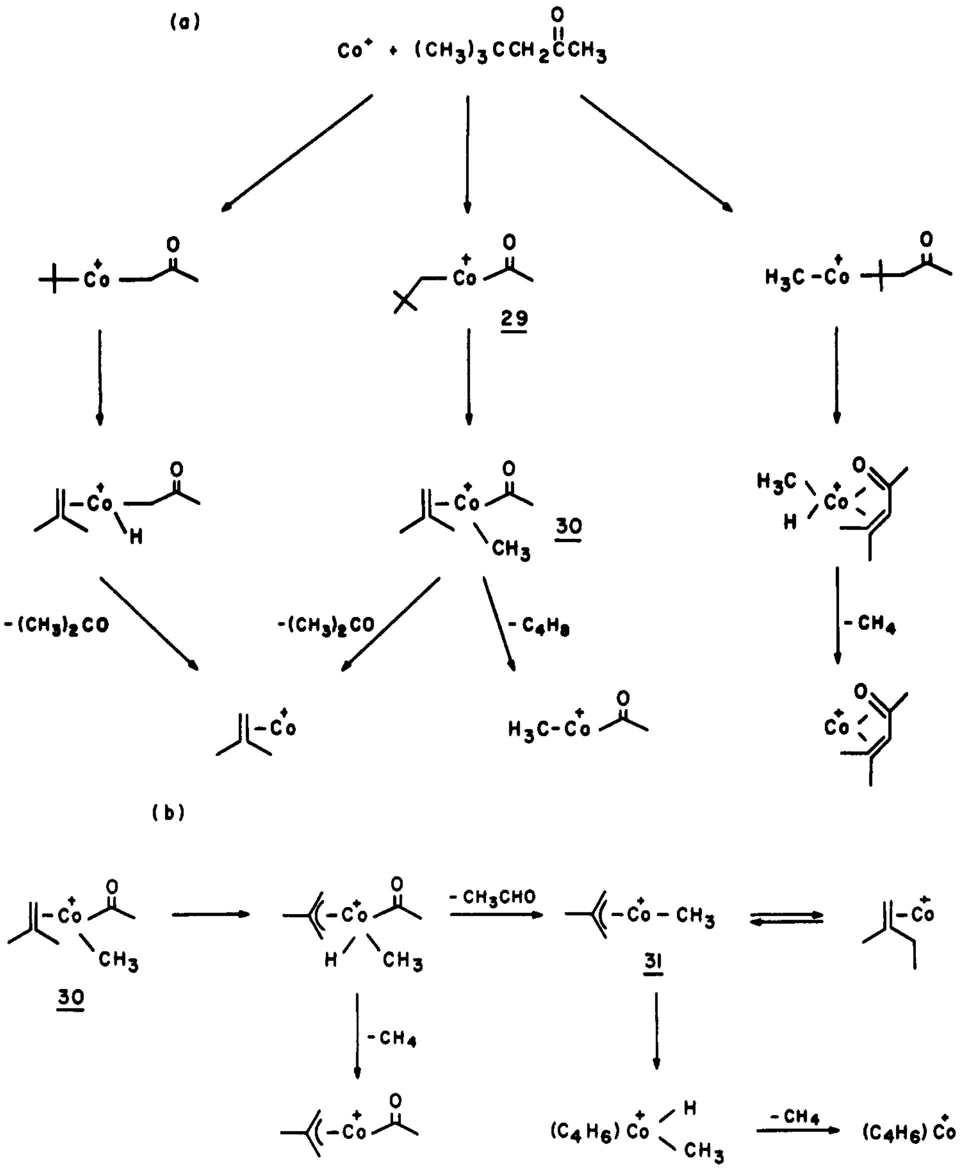

abstract an allylic hydrogen to form $\mathrm{Co(C_4H_6)^+}$. The latter product may also be formed by dehydrogenation of the $\mathrm{Co(C_4H_8)^+}$ ion (as in Scheme VI).

Cyclopentanone. The major products of the reaction of cobalt ions with cyclopentanone at low energies are loss of CO and loss of CO and $\mathrm{H_2}$ (eq 13 and 14).[39] These

$$\mathrm{Co^+} + \text{cyclopentanone} \rightarrow \mathrm{Co(C_4H_8)^+} + \mathrm{CO} \qquad (13)$$

$$\rightarrow \mathrm{Co(C_4H_6)^+} + (\mathrm{CO} + \mathrm{H_2}) \qquad (14)$$

products are formed in approximately equal amounts at very low relative kinetic energies, while the $\mathrm{Co(C_4H_6)^+}$ ion accounts for over 80% of the product distribution at slightly higher energies[40] (~1 eV). A small amount (~2% each) of loss of butene and $\mathrm{C_3H_4O}$ (see Table II) is also observed at low energies, with slightly larger amounts (~4% each) at 1 eV. The low-energy products were identified using cyclopentanone-α,α'-d_4.[39] At higher energies, a product with mass 101 appears, which corresponds to $\mathrm{Co(COCH_2)^+}$ or $\mathrm{Co(C_3H_6)^+}$.

The proposed pathway for loss of CO is similar to the previously described reactions with ketones. The metal ion inserts into the C–CO bond of cyclopentanone, followed by an alkyl shift onto the metal center. Ion cyclotron resonance spectroscopy experiments have shown that $\mathrm{M(C_4H_8)^+}$ ions, M = $\mathrm{Fe^+}$ and $\mathrm{Ni^+}$, formed from reaction of $\mathrm{M^+}$ with cyclopentanone are unreactive with HCN. This suggests the $\mathrm{C_4H_8}$ unit remains intact[6,10] for these two species. Similar studies were not done on the cobalt product. Reactions of $\mathrm{Fe^+}$, $\mathrm{Co^+}$, and $\mathrm{Ni^+}$ with cyclobutanone are reported to form metallacyclobutanes which, in the case of $\mathrm{Co^+}$ and $\mathrm{Ni^+}$, rearrange to propene–metal ion complexes.[41] In analogy to these systems, the decarbonylation process is expected to initially form the metallacyclopentane **32**. Subsequent dehydrogenation leads to the Co(1,3-butadiene)$^+$ ion. Cleavage of the metallacycle leads to loss of ethene.

The metallacyclopentane **32** has also been proposed as an intermediate in the reaction of $\mathrm{Co^+}$ with cyclobutane.[5]

---

[39] Studies of the reaction of $\mathrm{Co^+}$ with ^{18}O-labeled cyclopentanone indicate that decarbonylation is the major process in which a neutral of 28 amu using the unlabeled reactant is eliminated, accounting for greater than 90% of the product. A minor product results in loss of ethene from the 3,4 sites on the ring (Kalmbach, K. A.; Ridge, D. P., unpublished results). The neutral products of reaction 13 are uncertain. Possibilities are $\mathrm{H_2CO}$ or $\mathrm{H_2}$ + CO.

[40] Jacobson and Freiser have also examined the reactions of $\mathrm{Co^+}$ with cyclopentanone.[10b] The product distribution they resport is very similar to the one we observe at 1-eV relative kinetic energy.

[41] Jacobson, D. B.; Freiser, B. S. *Organometallics* **1984**, *3*, 513.

Scheme VIII

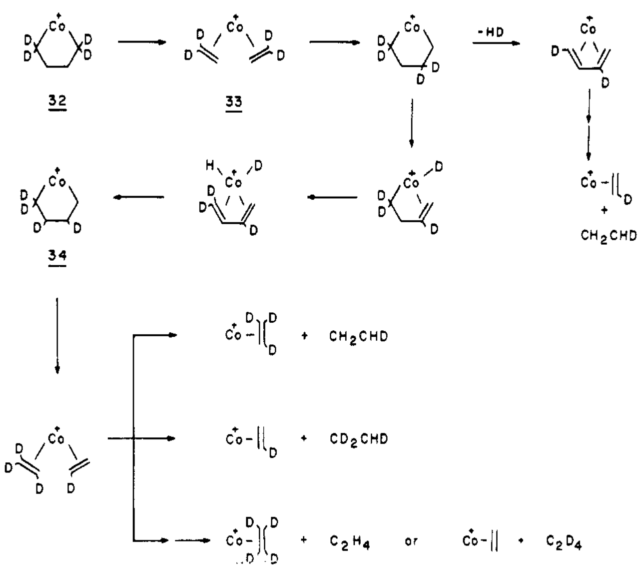

The major products of this reaction at low energies are dehydrogenation and loss of ethene (eq 15 and 16). The

$$Co^+ + c\text{-}C_4H_8 \longrightarrow \begin{cases} Co(C_4H_6)^+ + H_2 & (15) \\ Co(C_2H_4)^+ + C_2H_4 & (16) \end{cases}$$

ionic products of reactions 15 and 16 are the same as those observed in the reaction of Co^+ with cyclopentanone, which supports the supposition that **32** is a common intermediate in both reactions.

Studies using cyclopentanone-α,α'-d_4 indicate that some scrambling processes occur. For example, Scheme VIII predicts the Co(ethene)$^+$ ions from the labeled compound should be $Co(C_2H_2D_2)^+$. While this is the major Co(ethene)$^+$ product, the ions $Co(C_2H_3D)^+$,[42] $Co(C_2HD_3)^+$, and $Co(C_2D_4)^+$ are also observed with intensities ~14% that of the $Co(C_2H_2D_2)^+$ peak at 1.2-eV relative kinetic energy. A $Co(C_2H_4)^+$ product is also probably formed, but we cannot distinguish between this product and $Co(CO)^+$ which has the same mass. Scheme VIII proposes a possible mechanism to account for these products. The metallacycle **32**, shown to cleave to form a bis(ethene) complex, **33**, which may reform the metallacycle with one of the deuterated carbon atoms in the β-position. β-Hydrogen and β-deuterium then switch back and forth from carbon to metal center. At some point, the dehydrogenation or cleavage of the metallacycle with loss of ethene occurs. Thus, **34** can lead to both $Co(C_2H_3D)^+$ and $Co(C_2HD_3)^+$. Dehydrogenation of **34** may involve loss of H_2, HD, or D_2. In viewing the complexity of Scheme VIII, it is important to bear in mind that the Co(ethene)$^+$ species is a very minor product.[43]

The overall process for the reaction of Co^+ with cyclopentanone is analogous to that shown for acyclic ketones in Figure 3. Formation of the species corresponding to $R_1R_2Co^+$ is much more prominent in the cyclic ketone. This is presumably due to constraints imposed by the cyclic structure on the reductive elimination of R_1R_2 which, in this case, is the somewhat strained cyclobutane ring.

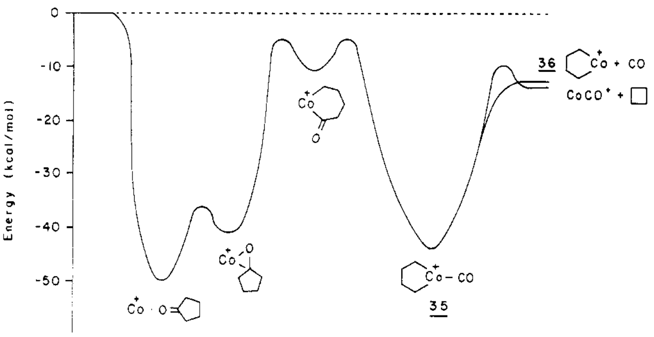

Figure 7. Simplified reaction coordinate diagram for the interaction of Co^+ with cyclopentanone.

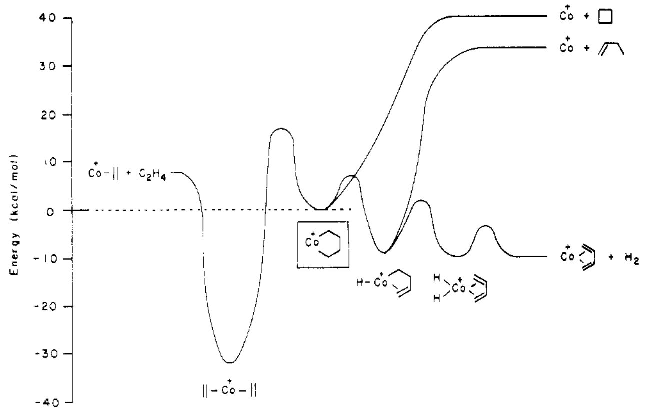

Figure 8. Simplified reaction coordinate diagram for decomposition of the metallacyclopentane formed in the interaction of Co^+ with cyclopentanone.

Moreover, the formation of the $R_1R_2Co^+$ product from reaction with cyclopentanone should be a more exothermic process. A semiquantitative potential energy diagram for the interaction of Co^+ with cyclopentanone is shown in Figures 7 and 8. Figure 7 is constructed by using arguments analogous to those used to discuss Figure 3, with the thermochemical estimates listed in Table VI. The decomposition of **35** to the metallacycle involves simple bond cleavage and is not expected to have much of an activation barrier. On the other hand, the reductive elimination of R_1R_2 to form $CoCO^+$ is expected to exhibit an activation barrier since the reverse process is not seen in the gas phase.[26]

A reaction coordinate diagram for the further decomposition of the metallacycle **36** is sketched in Figure 8. Dehydrogenation is the major product of this decomposition. Cleavage of the metallacycle to form $Co(C_2H_4)^+$ is shown as an endothermic process. The reverse reaction, addition of C_2H_4 to $M(C_2H_4)^+$ to form the metallacycle, would be detectable in gas-phase studies by the subsequent dehydrogenation that leads to the formation of $Co(C_4H_6)^+$. Examples of these olefin-coupling processes in solution are numerous.[44] However, ICR experiments designed to discover systems for which this reaction occurs in the gas phase, have not been successful.[45,46] This suggests an appreciable activation energy for metallacycle formation.

The diagram in Figure 8 predicts that reaction of Co^+ with cyclobutane and 1-butene will result in the formation

---

[42] This ion could also be partially due to loss of ethene in the reaction of Co^+ with cyclopentanone-α,α'-d_3, an impurity in our labeled compound.

[43] Interestingly, in the reactions of group 8 metal ions with alkanes, deuterium scrambling processes appeared to play a significant role only for Co^+ in contrast to Fe^+ and Ni^+.[2,35] Evidence for scrambling processes was also noted above for the reaction of Co^+ with 3-pentanone-α,α'-d_4 (Scheme V).

[44] Grubbs, R. H.; Miyashita, A. *J. Am. Chem. Soc.* **1978**, *100*, 1300. Stockis, A.; Hoffmann, R. *J. Am. Chem. Soc.* **1980**, *102*, 2952 and references therein.

[45] Hanratty, M. A.; Beauchamp, J. L., unpublished results.

[46] Only ligand displacement reactions were seen in the reactions of $Co(NO)(Co)_n^+$, n = 1–3, with C_2D_4. No olefin coupling reactions were observed: Weddle, G. H.; Allison, J.; Ridge, D. P. *J. Am. Chem. Soc.* **1977**, *99*, 105.

of $Co(C_4H_6)^+$ and $Co(C_2H_4)^+$. This is consistent with previously reported studies of these reactions.[4,5] While the diagram in Figure 8 is quite complex, it is not constructed to show every intermediate that may be involved. For example, a π-allyl complex is probably formed in the interaction of Co^+ with 1-butene.[4] This species is not shown in Figure 8.

Conclusion

The present results for the reactions of Co^+ with ketones and aldehydes complement and are in general agreement with the previous studies of Fe^+ by Freiser and co-workers (Table I).[9] The ability to vary kinetic energy in a quantitative fashion in the present study has provided additional insights into the mechanism and energetics of observed reactions. Using thermochemical data that have recently become available, we have attempted to construct reaction coordinate diagrams such as shown in Figures 3, 7, and 8, which are at least semiquantitative in describing reaction energetics.

Proposed reaction mechanisms for bare cobalt ions have close parallels in solution-phase studies of cobalt and rhodium complexes.[27,47-49] The known chemistry of rhodium(I) complexes is of particular interest since species have been identified which decarbonylate aldehydes.[27,47] Compared to metal complexes in solution, however, bare metal ions in the gas phase are very reactive, capable of disrupting a complex structure in a single bimolecular encounter. This destructive behavior results from a desire on the part of the metal ions to become ligated, a process which is achieved by converting complex aldehydes and ketones into smaller molecular fragments, including alkanes, alkenes, carbon monoxide, and hydrogen. It is clear, however, that insights into the synthesis of molecules can be gained by learning how they come apart and then considering what would be required to force the process in the reverse direction. For example, alkenes, hydrogen, and carbon monoxide can be assembled to form aldehydes (hydroformylation process) by using organometallic catalysts. Whereas group 8 metal ions oxidatively add to the C–CO bond of ketones (e.g., intermediates **1** or **8**), reductive elimination via $RH_2C{-}C(O)R$ bond coupling has been proposed to occur in the formation of ketones by reaction of acyl chlorides with alkylcobalt and alkylrhodium complexes.[48] While Co^+ forms alkenes in the reactions with ketones described above, it has been suggested that ethene may insert into the Rh–H bond of $RC(O){-}Rh(H)(PPh_3)_2Cl$ to generate $RC(O)C_2H_5$.[50] There are several salient features of the proposed reaction coordinate diagrams that relate to the possible formation of molecular species. Reaction of $Co(CH_3)_2^+$ with CO *may* lead to formation of acetone by moving to the left along the potential energy diagram shown in Figure 3. The system does not have sufficient energy for acetone to be released, however, and the only reaction path available to the system will be to move back to the right and reductively eliminate ethane. In fact, any experiment that started with a stabilized Co^+–acetone complex and added increasing amounts of excitation would result in formation of the decarbonylation products. Removal of acetone could be achieved by a ligand displacement reaction or by modifying the potential energy surface by attachment of spectator ligands that increase the activation energies for the initial step in the decarbonylation reaction.

Similar diagrams constructed for the reaction of Co^+ with cyclopentanone indicate that reaction of Co^+ with cyclobutane and 1-butene should yield $Co(C_2H_4)^+$ and $Co(C_4H_6)^+$. In fact, these processes are observed.[4,5] On the other hand, Figure 8 is constructed such that reaction of $Co(C_2H_4)^+$ with C_2H_4 will not yield the $Co(C_4H_6)^+$ ion. This conclusion is supported by unsuccessful searches for systems where this process occurs. For example, Ridge and co-workers have looked at the reactions of $Co(NO)(CO)_n^+$, $n = 1-3$, with C_2D_4.[46] Only ligand exchange reactions are observed. Similar results were reported by Jones and Staley for reactions of $CpCo^+$ with C_2D_4.[51] In analogy to the Co^+–acetone complex described above, at somewhat higher energies the Co^+–ethene adduct should be able to react with another molecule of ethene to form the metallacyclopentane. A high-pressure ion source, now being constructed for the beam apparatus, will allow us to generate these sorts of adducts and monitor the kinetic energy dependence of their reactions.

Acknowledgment. This research was supported in part by the U.S. Department of Energy. Graduate fellowship support from Bell Laboratories and the Shell Companies Foundation (L.F.H.) is gratefully acknowledged.

Appendix

While there is a growing collection of thermochemical data for organometallic compounds,[30,52,53] there are few data from systematic examination of bond strengths of M–CO, M–R, M–COR, $(R)_nM{-}CO$, etc. in gas- or condensed-phase studies.[54] Transferring values known for one system to another can be used only as a first approximation. With this background in mind, the thermochemical estimates used in sketching the potential energy diagrams in Figures 3, 7, and 8 are listed in Table VI. Some of the considerations involved in assigning these values are discussed below.

The binding energies of aldehydes and ketones to Co^+ are not known. Jones and Staley have studied the relative bond dissociation energies for two ligand complexes of Co^+, $\delta D(Co^+{-}2L)$, with several organic molecules, including acetone and acetaldehyde.[55] Plotting $D(CpNi^+{-}L)$,[56] where Cp = η^5-C_5H_5, vs. $\delta D(Co^+{-}2L)$, one obtains a line of slope ~0.5, suggesting that the difference in binding energy of various ligands to Co^+ and $CpNi^+$ is similar. The absolute values of the binding energies of acetone and acetaldehyde to $CpNi^+$ are known,[56] and the binding energies of formaldehyde and cyclopentanone to $CpNi^+$ can be predicted from their proton affinities.[56,57] These values are used as estimates for the binding energies of these compounds to Co^+, listed in Table VI. Because ketene is protonated on the methylene carbon rather than on oxygen,[58] its proton affinity will not be related to its binding

---

[47] Suggs, J. W. *J. Am. Chem. Soc.* **1978**, *100*, 640.

[48] Schwartz, J.; Cannon, J. B. *J. Am. Chem. Soc.* **1974**, *96*, 4721.

[49] An additional reaction of interest is the pyrolysis of acetyl complexes of the type $[PtXMe_2(COMe)L_2]$ (X = halogen; L = PMe_2Ph or $AsMe_2Ph$) that gives acetone and *trans*-$[PtXMeL_2]$ in quantitative yields. Ruddick, J. D.; Shaw, B. L. *J. Chem. Soc. A* **1969**, 2969.

[50] Lochow, C. F.; Miller, R. G. *J. Am. Chem. Soc.* **1976**, *98*, 1280.

[51] Jones, R. W.; Staley, R. H. *Int. J. Mass Spectrom. Ion Phys.* **1981**, *39*, 35.

[52] Halpern, J. *Acc. Chem. Res.* **1982**, *15*, 238.

[53] Martinho Simões, J. A.; Beauchamp, J. L., to be submitted for publication.

[54] Connor, J. A.; Zafarani-Moattar, M. T.; Bickerton, J.; El Saied, N. I.; Suradi, S.; Carson, R.; Al Takhin, G.; Skinner, H. A. *Organometallics* **1982**, *1*, 1166.

[55] Jones, R. W.; Staley, R. H. *J. Phys. Chem.* **1982**, *86*, 1387.

[56] Corderman, R. R.; Beauchamp, J. L. *J. Am. Chem. Soc.* **1976**, *98*, 3998.

[57] Aue, D. H.; Bowers, M. T. "Gas Phase Ion Chemistry"; Bowers, M. T., Ed.; Academic Press: New York, 1979; Vol. 2.

[58] Vogt, J.; Williamson, A. D.; Beauchamp, J. L. *J. Am. Chem. Soc.* **1978**, *100*, 3478.

energy to $\mathrm{CpNi^+}$ in a similar fashion. However, CO is not observed to displace ketene from $\mathrm{CpFe(CH_2CO)^+}$.[59] Thus, we assume $D[\mathrm{Co^+{-}(CH_2CO)}] > D[\mathrm{Co^+{-}CO}]$.

The two ligand binding energies to $\mathrm{Co^+}$ of the oxygen bases studied by Jones and Staley can also be correlated to binding energies to $\mathrm{Li^+}$.[55] The slope of the line in the correlation plot of $\mathrm{Li^+{-}L}$ binding energies vs. the relative dissociation enthalpy per ligand for $\mathrm{Co^+}$ of the oxygen base ligands, ethers, and alcohols, as well as ketones and aldehydes, is 1.10. This suggests that the mode of binding of the different ligands to $\mathrm{Co^+}$ is similar in character to the binding of these ligands to $\mathrm{Li^+}$. Calculations have shown that the $\mathrm{Li^+}$–base bond is basically electrostatic;[23] thus, $\mathrm{Li^+}$ binds to the lone pair on oxygen in these systems. Because of these considerations, the chemically activated species initially formed, structure **5** in Figure 3, is shown as binding end-on to the oxygen atom of the carbonyl group. Rearrangement can then lead to a π-bound complex.

The bond energies $D^0(\mathrm{Co^+{-}H})$ and $D^0(\mathrm{Co^+{-}CH_3})$ are known from previous ion beam studies.[2] Combining the methyl bond energy with the information that $D^0(\mathrm{Co^+{-}2CH_3}) > 96$ kcal/mol (see above) gives a lower limit of $D^0[\mathrm{(H_3C)Co^+{-}CH_3}] > 35$ kcal/mol. We have set $D^0[\mathrm{(H_3C)Co^+{-}CH_3}]$ equal to 40 kcal/mol. Because the polarizable methyl group stabilizes the metal cation more than H, $D^0[\mathrm{(H_3C)Co^+{-}CH_3}]$ will be smaller than $D^0[\mathrm{(H)Co^+{-}CH_3}]$. The latter is chosen to be 50 kcal/mol. Thus, $D^0[\mathrm{(H_3C)Co^+{-}H}] = 41$ kcal/mol and likewise should be less than $D^0[\mathrm{HCo^+{-}H}]$, to which a value of 50 kcal/mol is assigned.

Unfortunately, there are no estimates for binding energies of acyl and formyl groups to the gas-phase ions. On the basis of some condensed-phase studies, it has been suggested that metal alkyl and acyl bond energies are similar.[52,60-62] The acyl and formyl binding energies listed in Table VI are equal to the methyl bond energy estimates.

The binding energy of CO to cobalt ions has also not been measured. The binding energy of CO to $\mathrm{CpNi^+}$ is 40 kcal/mol.[63] Photoionization mass spectrometry studies have determined the appearance potentials for $\mathrm{Fe(CO)}_n^+$, $n = 1$–5, and $\mathrm{Ni(CO)}_n^+$, $n = 1$–4.[64] An average value for the binding energy of one CO to a metal ion from the above studies is ~40 kcal/mol. This value is listed in Table VI for $D[\mathrm{Co^+{-}CO}]$. This binding energy should decrease as more polarizable ligands are added onto the metal.

Additional, and more speculative, estimates used in constructing the diagrams in Figures 7 and 8 are also listed in Table VI. Because the ring strain in four- and five-membered metallacycles is often found to be small,[65] the binding energy for $\mathrm{(R_1R_2){-}Co^+}$, where $\mathrm{R_1R_2}$ is $\mathrm{\cdot CH_2(CH_2)CH_2\cdot}$, is estimated to be 5 kcal/mol less than $D[\mathrm{Co^+{-}2CH_3}]$.[66] Previous studies have determined a lower bound for the binding energy of ethene to $\mathrm{Co^+}$ of 36 kcal/mol.[4] The energies listed in Table VI reflect the fact that ethene is observed to displace CO in many gas-phase organometallic systems.[6,33,46,51] Because $\mathrm{Co(C_4H_6)^+}$ is not formed at low energies in the reaction of $\mathrm{Co^+}$ with *n*-butane,[2] the binding energy of $\mathrm{Co^+}$ to butadiene is suggested to be less than ~56 kcal/mol.[15]

Registry No. $\mathrm{H_2CO}$, 50-00-0; $\mathrm{CH_3CHO}$, 75-07-0; $\mathrm{(CH_3)_2CO}$, 67-64-1; $\mathrm{(CD_3)_2CO}$, 666-52-4; $\mathrm{CH_3CH_2COCH_3}$, 78-93-3; $\mathrm{CH_3CH_2COCD_3}$, 24313-50-6; $\mathrm{(C_2H_5)_2CO}$, 96-22-0; $\mathrm{(CH_3CD_2)_2CO}$, 6400-97-1; $\mathrm{(CH_3)_3CCOCH_3}$, 75-97-8; $\mathrm{(CH_3)_3CCH_2COCH_3}$, 590-50-1; $\mathrm{Co^+}$, 16610-75-6; $\mathrm{Fe^+}$, 14067-02-8; $\mathrm{Ni^+}$, 14903-34-5; cyclopentanone, 120-92-3; cyclopentanone-α,α'-d_4, 61363-26-6.

---

[59] Stevens, A. E.; Beauchamp, J. L. *J. Am. Chem. Soc.* **1978**, *100*, 2584.

[60] Yoneda, G.; Blake, D. M. *Inorg. Chem.* **1981**, *20*, 67. See also: Yoneda, G.; Lin, S.-M.; Wang, L.-P.; Blake, D. M. *J. Am. Chem. Soc.* **1981**, *103*, 5768.

[61] Brown, M. P.; Puddephatt, R. J.; Upton, C. C.; Lavington, S. W. *J. Chem. Soc., Dalton Trans.* **1974**, 1613.

[62] $D[\mathrm{R{-}Mn(CO)_5}]$ for R = $\mathrm{CH_3CO}$ has been determined to be ~6 kcal/mol greater than for R = $\mathrm{CH_3}$.[54]

[63] Corderman, R. R. Ph.D. Thesis, California Institute of Technology, 1977.

[64] Distefano, G. *J. Res. Natl. Bur. Stand., Sect. A* **1970**, *74*, 233. The $\mathrm{Fe^+{-}CO}$ bond energy is given as 2.62 ± 0.1 eV (60.5 ± 2 kcal/mol). This latter value may be too high. The threshold for formation of $\mathrm{FeCO^+}$ appears closer to 12.40 eV rather than 11.53 eV as suggested by Distefano. This lowers $D^0(\mathrm{Fe^+{-}CO})$ to 1.63 eV (37.6 kcal/mol).

[65] Moore, S. S.; DiCosimo, R.; Sowinski, A. F.; Whitesides, G. M. *J. Am. Chem. Soc.* **1981**, *103*, 948. Steigerwald, M. L.; Goddard, W. A., III, private communication.

[66] Estimates for $\Delta H_f(\mathrm{\cdot CH_2(CH_2)_2CH_2\cdot})$ are in the range of 61–67 kcal/mol; Doering, W. von E. *Proc. Natl. Acad. Sci. U.S.A.* **1981**, *78*, 5279. We have used a value of 62 kcal/mol in our calculations.